COBEM 2021 26th International Congress of Mechanical Engineering
November 22-26, 2021, Virtual Congress, Brazil
ABCM Associação Brasileira de Engenharia e Ciências Mecânicas

COB-2021-0093
NUMERICAL ANALYSIS OF ROLL WAVES GENERATION IN OPEN-CHANNEL FLOWS FOR A CONTROLLED PERTURBATION

Valdirene da Rosa Rocho
Guilherme Henrique Fiorot
Sergio Viçosa Möller
valdirene.rocho@ifc.edu.br
guilherme.fiorot@ufrgs.br
svmoller@ufrgs.br
Mechanical Engineering Graduate Program - PROMEC
Federal University of the Rio Grande of the Sul - UFRGS

Abstract. *This article brings a numerical work presenting results of two-phase flow of Newtonian fluids in a laminar, transient regime, evolving in an open channel, in conditions of propagation of roll wave instability. The simulations were performed using the OpenFOAM software, which uses the complete Navier-Stokes equations discretization by the finite volume technique. The fluids used in the numerical tests were glycerin and air for different entry conditions. In this work, more specifically, Euler schemes were employed for the time-derivative (CFL = 0.5), PIMPLE for the coupling of velocity pressure, and VoF technique (fluid of volume) to solve the interface. Firstly, the boundary conditions were specified in order to achieve the permanent and uniform regime for specific set of Froude and Reynolds numbers. Subsequently, a sinusoidal flow, with fixed frequency (3 Hz) and amplitude (15% of the uniform regime), was applied. Then, from the information of the fluid dynamic field, the generation and propagation of the roll waves was evaluated based on measurements at the interface of the following variables: position, longitudinal and transverse velocity. Data analysis was performed for different cases depending on the number of Froude. Finally, the following wave characteristics were identified: length, velocity, amplitude, maximum and minimum height. It was found that the stabilized waves are presented as long waves* ($^{\Delta h}/_{\lambda} << 1$)*, validating mathematical hypotheses used in shallow water modeling for simplifying mathematical models. It was noticed that the greater the Froude number, the greater the amplitude of the roll wave. Likewise, it was observed the wavelength also increases with the Froude number. Finally, for the simulated cases, it was possible to observe the necessary length for roll waves to establish and observe its dependency with the Froude number. Such measurement is of great interest for practical applications and should be further explored to promote finer tuning of numerical and theoretical models.*

Keywords: *Roll waves, Froude number, Perturbation frequency, Newtonian fluids.*

1. INTRODUCTION

Fluid flows are essentially interdisciplinary subjects in their nature, which possess broad areas of application, such as: flows through obstacles, geophysical (mud flows in sloping channels, slopes, among others), industrial, etc. The behavior of these flows is subject to various conditions, principles and laws, and can manifest themselves in a harmful way, depending on their characteristics, to civil infrastructures.

In specially, natural free surface flows are those that occur in inclined channels, with various fluids, of Newtonian or non-Newtonian nature, and may be laminar or turbulent, and yet multiphase and in multilayer, in which the driving force is usually the weight force of the fluid. If sufficient conditions are present, these flows may develop instabilities along their evolution in time and space (Needham and Merkin, 1984; Noble, 2007; Aktershev and Alekseenko, 2013), which increases the degree of unpredictability of the flow.

Such instabilities, which possess magnitude similar that of flow, they are capable of carry the devastating consequences. In mudflows, for example, they can be strong enough to cause serious damage to property. The rupture of dam B1 at the Córrego do Feijão Mine in Brumadinho in 2019, which caused a large avalanche of iron ore tailings, would be a scenario in which such instabilities could have been configured, although there are no records of their spatio-temporal evolution. Events of this type are marked in history and leave a trail of destruction and dozens of deaths when they occur, and the presence of instability could configure even greater damage.

Generally, these waves arise on the free surface of flows and propagate in the form of a train of waves. These waves have well-defined shapes, periodicity, and characteristic propagation velocity, and are thus called of roll waves. Thus, by identifying this phenomenon, its potential impact can be reduced, or even eliminated, through theoretical predictions

(D'Alessio and Pascal, 2008; Ferreira, 2013), for example.

The instabilities of the type roll wave (Fig. 1) then arise from the unbalance by various actions of the forces acting on the flow, gravitational and viscous, which, under the right conditions, amplify small perturbations and culminate in a well-defined wave on the free surface of the flow until it reaches a stable shape.

Figure 1: Examples of roll waves.

(a) Roll waves in a lateral irrigation canal, Cabana-Mañazo irrigation, Puno, Peru (2007).

(b) A typical experimental view of (a) developed roll waves, (b) a detailed view of a pair of waves, (c) merging waves at a downstream location, and (d) a stable flow.

Source: (a) Victor Miguel Ponce's personal online gallery at http://ponce.sdsu.edu/the-control-of-roll-waves.html; (b) Balmforth *et al.* (2004).

A theoretical-mathematical approach to obtaining information about roll waves was provided by Dressler (1949). In his theory, fixed parameters of channel geometry and flow conditions (slope, roughness, mean velocity) were given, and by employing a disturbance control parameter (wavelength) since it can be determined other wave characteristics: wave amplitude and celerity. Furthermore, Dressler (1949) found that roll waves occur only if the roughness of the channel base is non-zero and less than a certain critical value, as required by the instability criterion for a linearized disturbance.

The roll waves theory of Dressler (1949) was extended to laminar water flows by Ishihara *et al.* (1954), who also performed experiments on a thin water sheet. For laminar flow conditions, Ishihara *et al.* (1954) showed that the flow becomes unsteady as long as the Froude number exceeds a minimum value of 0.577. Such a condition is necessary but not sufficient for the formation of roll waves. In addition, the authors also check that there is a minimum channel length required for such instabilities to develop.

Extending the study of Ishihara *et al.* (1954), Tamada and Tougou (1979) evaluated the instability of roll waves in laminar flows from the formulation of the basic hydraulic equations that are derived from the assumptions of long waves and parabolic velocity profile. In addition, they numerically solved an eigenvalue problem to determine the length of these waves, in which they searched for the "most stable" wavelength. Their mathematical procedure, however, was not clear enough to be convincing.

Later, seeking to quantify this phenomenon, Julien and Hartley (1986) studied the roll wave event in laminar flow under smoothly inclined channel, both numerically and experimentally in subcritical flows, in order to evaluate the length required for its formation, as well as velocity and frequency. They also analyzed the stability of roll waves by means of the Vedernikov number (Ve).

Posteriorly, the study of roll waves was generalized to fluids with more complex rheology, such as power-law (Ng and Mei, 1994), Bingham (Liu and Mei, 1994), and Herschel-Bulkley (Maciel *et al.*, 2013). Subsequent, In the attempt to better represent the modeling of roll waves type flows, many researchers seek to improve analytical models and measure physical manifestations of these[1], such as Balmforth *et al.* (2004), D'Alessio and Pascal (2008), Fiorot *et al.* (2015), Di Cristo *et al.* (2010), among many others, with the objective to validate models.

Within this context, this paper presents the investigation on the generation of roll waves in laminar flow evolving in an open channel, through numerical experiments developed in OpenFOAM software. Perturbations of sinusoidal type are made over a developed free surface flow and the evolution of such perturbations into roll waves is evaluated. The main roll waves characteristics are evaluated, such as: length, velocity, amplitude, maximum and minimum height, as well as the relative amplitude with respect to the height of the flow in permanent regime. Furthermore, we seek to obtain an estimate of the channel length needed to be walked by these waves until they become stable, given a constant frequency perturbation.

[1]Experimental results of roll waves in different configurations are still scarce in the literature.

2. Metodology

This item describes the physical roll wave problem and the numerical methodology for modeling the two-dimensional flow of Newtonian fluid in a transient, laminar and incompressible regime, by the conservation equations for linear mass and momentum.

2.1 Roll waves instabilities

The roll wave problem aim of the present study is established on the free-surface flow (plane Poiseuille flow), for a Newtonian fluid. Solving the conservation equations (mass and momentum) for such problem in steady and uniform regime, one obtains the following:

- **velocity profile:**

$$u(y) = -\frac{h_0^2}{2}\left(\frac{\rho g \sin\theta}{\mu}\right)\left[1-\left(1-\frac{y}{h_0}\right)^2\right] = \left(\frac{\rho g \sin\theta}{\mu}\right)\left(\frac{y^2}{2}-h_0 y\right), \tag{1}$$

- **free-surface velocity:**

$$u(h_0) = -\frac{h_0^2}{2}\left(\frac{\rho g \sin\alpha}{\mu}\right), \tag{2}$$

- **mean flow velocity:**

$$u_0 = \frac{h_0^2}{3}\left(\frac{\rho g \sin\theta}{\mu}\right), \tag{3}$$

- **unit discharge:**

$$q = \frac{h_0^3}{3}\left(\frac{\rho g \sin\theta}{\mu}\right), \tag{4}$$

where h_0 is the mean flow height, y is the vertical coordinate, ρ the fluid density, μ dynamic viscosity, g gravity acceleration and θ the channel slope.

Another important parameter that needs to be considered for this analysis is the wave propagation velocity U, also called group velocity (Ng and Mei, 1994; Rocho *et al.*, 2020):

$$\frac{U}{u_0} = \alpha + \sqrt{\alpha^2 - \alpha + \frac{1}{Fr^2}} \tag{5}$$

where α is the momentum distribution over the vertical coordinate (for Newtonian fluid $\alpha = 1.2$), and Fr is the Froude number, calculated as given by Eq. (6):

$$Fr = \frac{u_0}{\sqrt{g h_0 \cos\theta}}. \tag{6}$$

The roll waves appearance in this kind of flow depend on the hydraulic regime of the flow. As established in the literature and mentioned before (Ishihara *et al.*, 1954; Julien and Hartley, 1986), for roll waves to appear $Fr > 1/\sqrt{3}$. Linear stability analysis shows that disturbances characterized as small-amplitude waves ($a << h_0$) with wavenumber k and frequency ω grow in space and time, culminating in a established roll wave pattern, as illustrates Fig. 2.

In Fig. 2 it is possible to see the flow properties as defined by the previous equations for the flow showing a 2D velocity field (u, w). Also, Fig. 2 shows the properties of the waves such as the wave crest (maximum height) $h_{\max}$, wave trough (minimum height) $h_{\min}$, and wavelength λ. It is expected that to reach the established configuration, waves must travel a minimum longitudinal distance L_{rw}. Di Cristo *et al.* (2010) studied such problem for infinitesimal flow disturbances and showed it was possible to estimate the length required for those waves to reach steady configuration (Fiorot *et al.*, 2015), as shows Eq. (7).

$$L_{\min} = \ln\eta\left[\frac{u_0^2}{g\sin\theta}\right]\left[\frac{2(Fr+1)}{Fr(Fr-2)\cos\theta}\right], \quad \text{with } \eta = 10^{-4}. \tag{7}$$

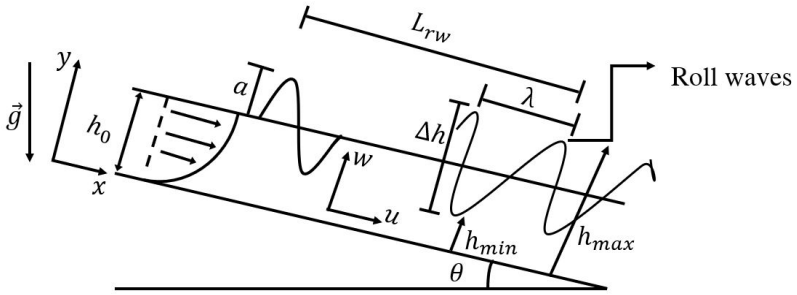

Figure 2: Schematic representation of free-surface flow.

2.2 Numerical modeling

The results presented in this paper come from mathematical modeling of the conservation and linear momentum equations under the imposition of a perturbation in the boundary conditions on the inlet velocity, in order to obtain the flow in the configuration of roll wave and then evaluate its main features.

The numerical implementation was performed in OpenFOAM software and post-processed in MATLAB® software. For the planning and execution of the simulations, the following steps were elaborated:

1. determination of the minimum channel length for obtaining roll waves;
2. where h_0 m is the height of the liquid layer, the height of the gas layer was defined as $20h_0$, the sum of which being the total dimension of the numerical domain in y;
3. creation of a structured two-dimensional mesh with standard refinement, in which a fixed dimension is used for each control volume, where $\Delta x/L = 10^{-3}$ and $\Delta y = {}^{1}/_{5}\Delta x$;
4. definition of input parameters: average velocity, flow rate, specific mass, kinematic viscosity, surface tension, rheological parameters and channel slope θ;
5. choice and adaptation ot the numerical schemes from the `dambreak` tutorial, available in the OpenFOAM tutorials;
6. definition of boundary and initial conditions.

From these steps, two cases of two-phase flow were studied, via two strands:

- **Case 1** – permanent and uniform flow;
- **Case 2** – imposition of a sinusoidal-type flow inlet perturbation (Eq. (8)):

$$u = u_0 \left[1 + a \sin(2\pi f t)\right] \tag{8}$$

where a is the amplitude and f is the frequency.

The numerical technique used in this work to discretize the conservation equations was finite volumes technique, which is based on the integration of differential equations into discrete control volumes. In this perspective, the complete Navier-Stokes equations are solved (Versteeg and Malalasekera, 1995; Fortuna, 2000).

To solve the interface problem, the VoF (Volume of fluids) method was used, which allows detecting the interface between the two fluids by calculating the volume fraction, which evolves from 0 (gas) to 1 (liquid), and makes it possible to identify the free surface that is located on the 0.5 level curve. The VoF method is widely applied in the simulation of two-phase flows involving immiscible phases, because mass is conserved.

To calculate the pressure, the solver used was the PIMPLE algorithm, which uses the PISO correction number in each step in time, and also uses the SIMPLE relaxation factor for pressure correction, which assist to maintain the compatibility of conservative equations, producing faster results, with a smooth and convergent behavior until permanent regime is reached (Gomes, 2015; Fernandes, 2017; Greenshields, 2019).

For the boundary conditions for the problem, Dirichlet boundary conditions were used, to prescribe fixed values of interest and Neumann's to preserve the flow of properties. Table 1 describes the conditions used in the simulations for **Case 1**.

For the initial conditions of the problem, the velocity field of the flow was defined, which is assumed to be the value of the average velocity of the flow, determined from Eq. (3).

Table 1: Boundary conditions for **Case 1** regarding p, $\mathbf{u}$ e α.

Boundary conditions	p $(^{N}/_{m^2})$	$\mathbf{u}$ $(^{m}/_{s})$	α
Inlet gas	$^{\partial p}/_{\partial n} = 0$	$^{\partial \mathbf{u}}/_{\partial \mathbf{n}} = 0$	0
Inlet liquid	$^{\partial p}/_{\partial n} = 0$	$^{\partial \mathbf{u}}/_{\partial \mathbf{n}} = 0$	1
Top	$^{\partial p}/_{\partial n} = 0$, for positive flow, or $p = 0$ flow is negative	$^{\partial \mathbf{u}}/_{\partial \mathbf{n}} = 0$, for positive flow, or $\mathbf{u} = 0$ flow is negative	$^{\partial \alpha}/_{\partial n} = 0$, for positive flow, or $\alpha = 0$ flow is negative
Bottom	$^{\partial p}/_{\partial n} = 0$	$\mathbf{u} = 0 = 0$	$^{\partial \alpha}/_{\partial n} = 0$
Outlet	$p_p = p_0 - 0.5\|U\|^2$	$^{\partial \mathbf{u}}/_{\partial \mathbf{n}} = 0$	$^{\partial \alpha}/_{\partial n} = 0$

Since it is dealing with a transient problem, a maximum time interval was defined for $\Delta t = 0.001$ s, that is, the time step used by the software to realize the calculations. The time interval is adjusted at the beginning of the loop of each iteration, using Courant's number relation, which relates the spatial and temporal dimensions of the simulation:

$$Co = \frac{\Delta t}{\Delta x}|u| < 0.5, \tag{9}$$

where $|u|$ is the norm of the local velocity magnitude, Δt the time step, and Δx the local size of a control volume of the mesh.

It is stands out that this one must be small enough to resolve for all time-dependent properties, i.e. the stability of the solution procedure is often controlled by an adaptive time step. Typically, the physical simulation times for cases 1 and 2 were 30 and 10 seconds, respectively.

For the validation of the methodology, the data from experimental tests (Tab. 2) of a glycerine flow ($\rho = 1237$ $^{kg}/_{m^3}$, $\nu = 1.71 \times 10^{-4}$ $^{kg}/_{ms}$) over an inclined plane of Fiorot *et al.* (2015) was used. For all tests that will be performed, the gas phase will be air ($\rho = 1$ $^{kg}/_{m^3}$, $\nu = 1.48 \times 10^{-5}$ $^{kg}/_{ms}$). The superficial tension is $\sigma = 0.07$ $^{N}/_{m}$.

Table 2: Experimental results for fixed slope channel ($\theta = 8°$).

Test	q $(^{l}/_{ms})$	μ $(^{kg}/_{ms})$	h_0 (mm)	u_0 $(^{m}/_{s})$	Fr
1	0.75	0.2120	9.832	0.2558	0.83
2	0.96	0.2173	10.726	0.2981	0.92
3	1.14	0.2117	11.566	0.3282	0.98

Source: Adapted from Fiorot *et al.* (2015).

After the certification of the numerical results, simulations were elaborated varying the Froude number from the variation of the flow rate, fixing the properties of the fluid ($\mu = 0.212$ $^{kg}/_{ms}$, $\rho = 1237$ $^{kg}/_{ms^3}$). Next, Tab. 3 with the essential parameters for the execution of the numerical tests was prepared.

Table 3: Numerical test data from the simulation with an inclined channel at $\theta = 8^o$.

Test	q $(^{l}/_{ms})$	h_0 (mm)	u_0 $(^{m}/_{s})$	Fr
4	0.87	6.885	0.1259	0.49
5	1.1	7.451	0.1476	0.55
6	1.57	8.387	0.1868	0.65
7	2.00	9.098	0.2198	0.74
8	3.80	11.362	0.3344	1.00
9	4.60	12.009	0.3830	1.12
10	5.70	12.925	0.4436	1.25
11	6.77	13.680	0.4946	1.36

For **Case 2**, from the validated solution of the tests performed in **Case 1**, the input boundary condition was varied and then a perturbation (Eq. (8)) was applied, with the following values to each parameter: $a = 0.15$ and $f = 3$ Hz.

2.3 Interface properties

The post-processing of the informations was executed in MATLAB® software, aiming to discuss the numerical results about the roll waves evolution. Routines were developed to search for information about the flow properties at the interface ($\alpha = 0.5$).

To identify the roll waves from the interface, the theory of cubic interpolation was aplied , which is a method that allows finding approximate values for a function at some point $P(x, y)$ of the domain. Regarding the numerical interpolation process, the integral function was used, in which it is defined that every curve between two adjacent points consists of a third order polynomial.

The roll wave characteristics were evaluated principally when they become stable (constant amplitude). A routine was developed in MATLAB® to determine the points of local maximum and minimum along the domain, which represents the maximum ($h_{\max}$) and minimum ($h_{\min}$) wave heights. From these measures, the wavelength (λ), amplitude (Δh), and the length traveled by the roll waves along the channel until they become stable (L_{rw}) can also be determined.

In particular, to determine L_{rw}, for each time instant, we first looked for two asymptotic curves interpolated over the local maxima and minima previously defined. Next, the difference between these two curves was calculated, thus defining an interpolated curve for Δh. Subsequently, we sought to determine the derivative of Δh and find the critical point at x of the function, which will be L_{rw}, being this the place where the function reaches a maximum point, due to the fact that Δh has asymptotic behavior, the slope of the tangent line at this location is null, that is, it is a constant function.

3. Results and discussions

In this first result, the first three tests performed for validation of the two-phase model are presented (Tab. 2). For confrontation of the results, we evaluated the **Case 1** for the expected analytical $u(y)$ velocity profile, employing the mean relative error. The numerical-analytical confrontation was done for the Poiseuille case, which presented good results, with numerical error around 0.14%. Also, since the kinematic and dynamic characteristics of the interface have great relevance for this study, the velocity at the free surface was also evaluated for the cases studied, and it was found that the relative error was less than 0.12%.

After confirming the good response for the **Case 1** model, we leave on to evaluate the **Case 2**, of the perturbed two-phase flow. Figure 3, illustrates the profile of the roll waves obtained from the simulation with the parameters set as Test 1 in Tab. 2.

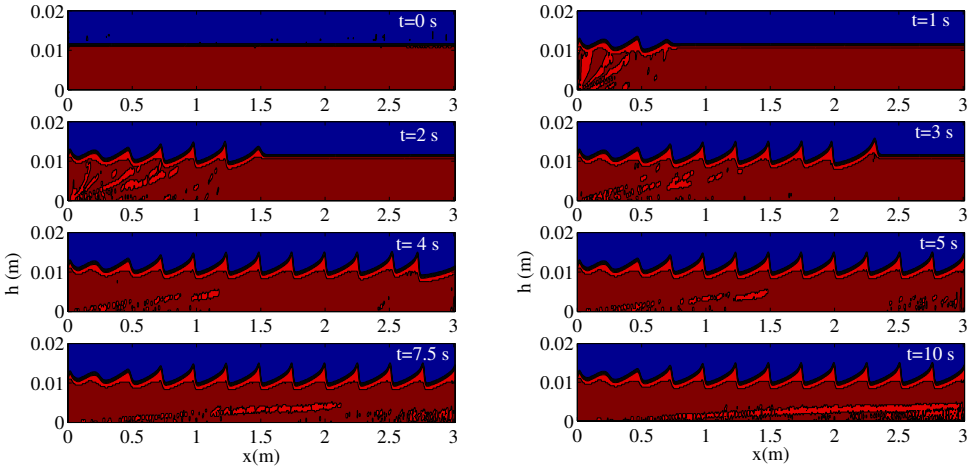

Figure 3: Multiphase flow developed in a channel for $Fr = 0.83$, for different time steps: $t = 0$, 1.0, 2.0, 3.0, 4.0, 5.0, 7.5, and 10.0 s, respectively. The reddish colors indicates the liquid phase, and the blueish color the gas phase.

It can be observed by means of Fig. 3, the spatial-temporal evolution of the perturbation made upstream, at the fixed point $x = 0$. It can be seen that the perturbations, sinusoidal, advance in the flow domain, and grow. Indeed, the same they appear to become stable from about $t = 5$ s, where the wave train starts having a periodic behavior, with well-defined amplitude and waves of the same length.

In the second part of the results, we seek to investigate the effect of Froude number on the generation and propagation of roll waves in a spatial analysis. From the interface detection algorithms, we represent the height of the liquid sheet as a function of the spatial coordinate x by means of Figs. 4 (a) and (b). Such results identify the profile of the roll waves for different Fr, generated by the applied perturbation.

In relation to Fig. 4, it is stands out that for the tests in which $Fr < Fr_{\min}$, the roll waves attenuate as predicted by the literature. For the tests in which $Fr > Fr_{\min}$, one notices that as we increase the Froude number, we have an increase in the amplitude Δh. Another observation that can be made, is that there is also an increase in the wavelength λ. It is worth noting that Fiorot *et al.* (2015) makes the same observations in his practical experiments.

In the Tab. 4 displays the results of the roll wave properties extracted from the numerical tests for the cases where the waves propagate in space.

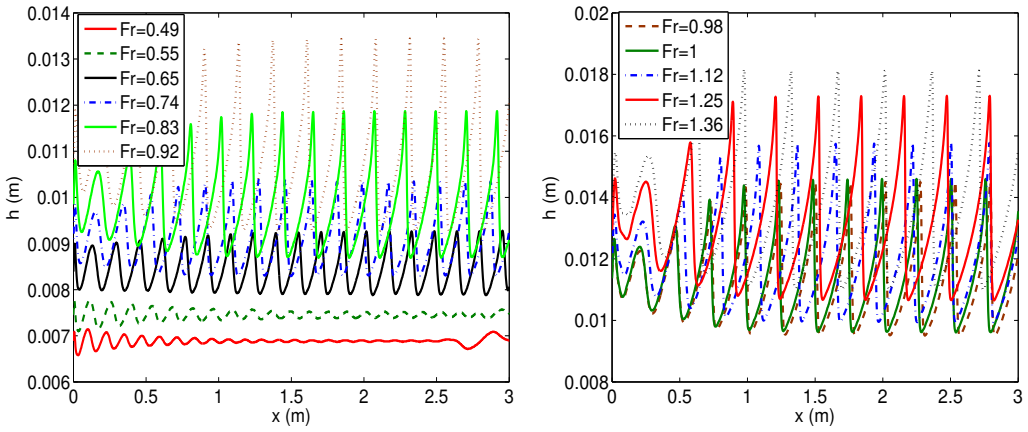

(a) (b)

Figure 4: Roll wave profile in the permanent regime for different Froude numbers, equal and constant amplitudes.

Table 4: Geometric properties of roll wave properties for different Froude numbers for $Fr > Fr_{\min}$.

Fr	λ (m)	Δh (mm)	$h_{\max}$ (mm)	$h_{\min}$ (mm)
0.65	0.154	1.3963	9.2772	7.8809
0.74	0.177	2.1075	10.4035	8.2960
0.83	0.212	3.1774	11.8684	8.6910
0.92	0.235	4.1667	13.4415	9.2748
0.98	0.258	5.0045	14.5120	9.5075
1.00	0.255	4.9906	14.6003	9.6098
1.12	0.283	5.8346	15.7706	9.9360
1.25	0.317	6.6552	17.3035	10.6483
1.36	0.347	7.1633	18.1653	11.0019

In the with respect to the approximate value for the wavelength for different Froude numbers, it can be concluded that we have long waves ($\Delta h << \lambda$), which is typical for fluid flows in shallow water. Also, it can be seen that as we increase the depth of the flow (height of the liquid sheet) the wave amplitude becomes larger (Ferreira, 2013; Fiorot *et al.*, 2015).

The same way the interface position is used to identify the geometric greatness of the roll waves, one can employ the same wave analysis with respect to the longitudinal u and transverse w velocity profiles of the free surface.

In the Tab. 5 thus displays the kinematic properties of the interface, presenting the propagation velocity of the roll waves (numerical and analytical (Eq. (5)), as well as the amplitudes, and minimum and maximum values for the velocities.

Table 5: Roll wave velocity properties in $^{m}/_{s}$ for different Froude numbers.

Fr	$U = \lambda \cdot f$	U (Eq. 5)	Δu	Δw	$u_{\max}$	$u_{\min}$	$w_{\max}$	$w_{\min}$
0.65	0.462	0.5059	0.1306	0.0351	0.3140	0.1834	0.0224	-0.0038
0.74	0.529	0.5555	0.1734	0.0299	0.3876	0.2142	0.0231	-0.0068
0.83	0.639	0.6106	0.1499	0.0504	0.4687	0.2772	0.0404	-0.0100
0.92	0.705	0.6781	0.1934	0.0684	0.5537	0.3225	0.0559	-0.0125
0.98	0.774	0.7260	0.2408	0.0823	0.6397	0.3558	0.0695	-0.0128
1.00	0.765	0.7333	0.3088	0.0823	0.6322	0.3234	0.0651	-0.0124
1.12	0.849	0.8018	0.3732	0.0915	0.7434	0.3702	0.0799	-0.0116
1.25	0.951	0.8910	0.4460	0.1042	0.8744	0.4284	0.0914	-0.0128
1.36	1.041	0.9647	0.5267	0.1113	1.0049	0.4782	0.0970	-0.0143

Regarding the wavelength, we obtain the same values already identified in Tab. 4 and also a relative error around 4.3% in relation to the velocity of propagation of the numerical and analytical roll waves.

In the third part of this paper we tried to evaluate the distance that the fluid must travel to form stable roll waves. We conjectured through the Fig. 4 that from a certain point in the domain the amplitude of these waves does not change. Thus, we sought to define a mathematical relationship between the Froude number and this distance traveled by the roll waves, which we named L_{rw}.

For the determination of L_{rw} we use the concepts of derivative, and evaluate when it is null, that is, we obtain the critical point of the function, and it is at this point that the function reaches its maximum. In this paper, we consider the derivative to be null, when we obtain a value of the order of 10^{-4}. Therefore, we consider that the distance L_{rw} that perturbations travel in the domain in the horizontal direction until they reach the critical point is the length that these waves need to travel to become stable roll waves. Indeed, the Tab. 6 brings up these values.

Table 6: Length required for roll waves establishment for different Froude numbers.

Fr	0.65	0.74	0.83	0.92	0.98	1.00	1.12	1.25	1.36
L_{rw} (m)	1.48	1.60	1.77	1.89	2.00	2.03	2.05	2.07	2.08
L^*_{rw}	18.03	11.61	9.92	8.71	7.77	8.20	6.83	5.76	4.99

From Tab. 6, it can be seen that the distance required for perturbations to travel until they become stable roll waves increase with Froude number, i.e., perturbations travel a longer distance to become stable. This fact can be justified as a consequence of the flow rate. By increasing Fr, automatically the amount of fluid flowing through the channel also increases, then the flow increases its inertial capacity, or advective, carrying the flow properties more easily, causing the disturbances to travel a greater space in the domain to stabilize.

Also, in order to evaluate the length L_{rw} as a function of the generated roll wave characteristics, it was treated the dimensionless form $L^*_{\text{rw}} = {}^{L_{\text{rw}}}/_{\lambda}$. Such results are presented in Tab. 6 which brings the L^*_{rw} lengths for each test.

From the data set displayed in the Tab. 6, it can be seen that the dimensionless length necessary to the establishment of the roll waves is smaller the higher the Froude number. Such variation does not follow exactly the same behavior of λ with Fr, which points to the particular influence of the dynamics of the flow on the evolution of instabilities. We illustrate in Fig. 5 the scatter diagram that corresponds to the relationship between Froude number versus L^*_{rw} and also the curve that best fits these points. For such modeling, the nonlinear least squares method (LSM) fitting utility of MATLAB® with the Least Absolute Residual (LAR) method was used.

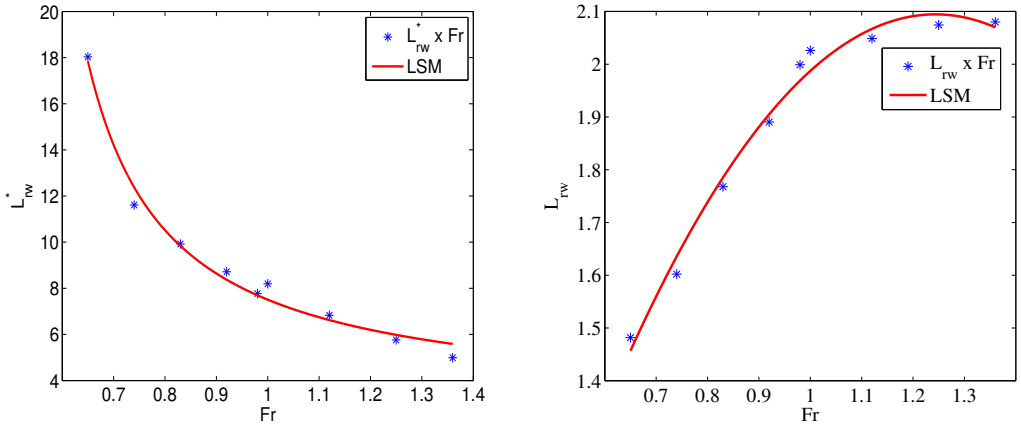

(a) L^*_{rw} as function of Fr for the numerical tests performed. (b) L^*_{rw} as function of Fr for the numerical tests performed.

Figure 5: Graphics of the length required for roll waves establishment for different Froude numbers.

The resulting function that best fitted the behavior is represented by a mathematical relationship of the rational type being these:

$$f(x) = \frac{2.89x + 0.91}{x + 0.49} \tag{10}$$

and

$$g(x) = -1.81x^2 + 4.502x - 0.7043 \tag{11}$$

the Eq. (10) refers to the function that best fits the set of points represented by the scatter diagram of Fig. 5(a) and Eq. (11) the function of Fig. 5(b), respectively. Both with R^2 of the order 99%.

4. Conclusion

In this paper, the formation of roll waves in laminar flows in the steady regime is studied from the complete Navier-Stokes equations with 2D flows, they are examined by means of a numerical analysis supported by experimental data from

Fiorot *et al.* (2015). The numerical simulations then confirm the existence of well-known hydrodynamic instabilities, the so-called roll waves, which are located at the fluid interface.

It is considered that the use of numerical simulation via OpenFOAM software is very consistent with the experimental results of Ferreira (2013) and Fiorot *et al.* (2015), such as: wavelength, velocity and principally of period. And yet, when dealing with flow in a uniform steady state, without imposition of perturbation, they were validated via literature and an error around 0.14% is obtained.

From the illustrations (tables and graphs) presented throughout this paper, it was noted that the 2D mathematical model represented well the roll waves and it can be verified that the Froude number is one of the parameters responsible for controlling the existence or not of roll waves. It is worth noting that, the geometric and kinematic characteristics of the interface representing the wave are dependent on the magnitude of the flow as a function of Fr. In particular, it is also noted that as we increase the height of the blade the waves become even longer.

With relation to the establishment length of roll waves L_{rw}, one can conclude that the Froude number is a factor controller of the amplification and influences in the necessary horizontal distance that perturbations need to travel before settling as stable roll waves. Such a distance seems to increase with Fr, dimensionally, however a dimensionless analysis as a function of wavelength points to a shorter establishment with increasing Fr.

And yet, in this paper it was possible, from the results, to obtain interpolating functions to predict the distance necessary to establish roll waves as a function of the Froude number, with good approximation since the correlation coefficient obtained was of the order of $R^2 = 0.99$.

5. ACKNOWLEDGEMENTS

The author of this paper thanks the Sombrio Advanced Campus of the Catarinense Federal Institute for granting a full time leave for doctoral studies, via notice nº 21/2019. In particular, the author would like to thank the IFC Dean's Office, which made possible to use a computer lab with the OpenFOAM software installed. This resource was of paramount importance for carrying out the numerical simulations that resulted in this study.

6. REFERENCES

Aktershev, S. and Alekseenko, S., 2013. "Nonlinear waves and heat transfer in a falling film of condensate". *Physics of Fluids*, Vol. 25.

Balmforth, N.J., Bush, J.W.M. and Craster, R.V., 2004. "Rolling on custard". pp. 1–5. URL `https://www.math.ubc.ca/ njb/Research/custard.pdf`.

D'Alessio, S.J.D. and Pascal, J.P., 2008. "A mathematical and numerical study of roll waves". *WIT Transactions on Engineering Sciences*, Vol. 59, pp. 1–10.

Di Cristo, C., Iervolino, M., Vacca, A. and Zanuttigh, B., 2010. "Minimum channel length for roll-wave generation". *Journal of Hydraulic Research*, Vol. 04, pp. 73–79.

Dressler, R.F., 1949. "Mathematical solution of the roll-waves in inclined open channels". *Communications on Pure and Aplied Mathematics*, Vol. 2, pp. 149–194.

Fernandes, P.C.G., 2017. "Estudo por simulação de cfd do efeito de pressurização-aspiração em bocal sônico e supersônico".

Ferreira, F.O., 2013. *Estabilidade e controle dinâmico de roll waves.* Doutorado em engenharia elétrica, Universidade Estadual Paulista - UNESP, Ilha Solteira/SP.

Fiorot, G., Maciel, G., Cunha, E. and Kitano, C., 2015. "Experimental setup for measuring roll waves on laminar open channel flows". *Flow Measurement and Instrumentation*, Vol. 41, pp. 149 – 157. ISSN 0955-5986.

Fortuna, A.O., 2000. *Técnicas Computacionais para Dinâmica dos Fluidos: Conceitos Básicos e Aplicações*.

Gomes, L.A.C.N., 2015. *Estudo da Transferência de Calor por Convecção Natural em Dissipadores Usando OpenFoam*. Mestrado em engenharia mecânica, Universidade Federal de Itajubá, Itajubá.

Greenshields, C.J., 2019. *User Guide*. The OpenFOAM Foundation LTda, 7th edition. URL `https://openfoam.org`.

Ishihara, T., Iwagaki, Y. and Iwasa, Y., 1954. "Theory of roll waves trains in laminar water flow on a steep slope surface." *Transactions of the Japan Society of Civil Engineers*, Vol. 1954, No. 19, pp. 46–57.

Julien, P.Y. and Hartley, D.M., 1986. "Formation of roll waves in laminar sheet flow". *Journal of Hydraulic Research*, Vol. 24, No. 1, pp. 5–17.

Liu, K.F. and Mei, C.C., 1994. "Roll waves on a layer of a muddy fluid flowing down a gentle slope — a bingham model".

Maciel, G., Ferreira, F. and Fiorot, G., 2013. "Control of instabilities in non-newtonian free surface fluid flows". *Journal of the Brazilian Society of Mechanical Sciences and Engineering*. doi:10.1007/s40430-013-0025-y.

Needham, D.J. and Merkin, H., 1984. "On roll waves down an open inclined channel". *Journal Mathematical physical & engineering sciences*, Vol. 394, pp. 259–278.

Ng, C.O. and Mei, C.C., 1994. "Roll waves on a shallow layer of mud modelled as a power-law fluid". *Journal of Fluid Mechanics*, Vol. 263, p. 151–184.

Noble, P., 2007. "Linear stability of viscous roll waves". *Communications in Partial Differential Equations - COMMUN PART DIFF EQUAT*, Vol. 32, pp. 1681–1713.

Rocho, V.R., Fiorot, G.H. and Möller, S.V., 2020. "Linear stability analysis of non-newtonian free surface flows a mathematical study on the temporal and spatial branches". *Annals of 18th Brazilian Congress of Thermal Sciences and Engineering*. URL https://abcm.org.br/proceedings/view/CIT20/0197.

Tamada, K. and Tougou, H., 1979. "Stability of roll-waves on thin laminar flow down an inclined plane wall".

Versteeg, H.K. and Malalasekera, W., 1995. *An introduction to computational fluid dynamics: the finite volume method.* Longman Scientific Technical, New York.

7. RESPONSIBILITY NOTICE

The authors are the only responsible for the printed material included in this paper.